Progress in Physical Geography 27,1 (2003) pp. 69–87

A review of rockfall mechanics and modelling approaches

Luuk K.A. Dorren

Institute for Biodiversity and Ecosystem Dynamics, Universiteit van Amsterdam, Nieuwe Achtergracht 166, NL-1018 WV Amsterdam, the Netherlands

Abstract: Models can be useful tools to assess the risk posed by rockfall throughout relatively large mountainous areas (>500 km^2), in order to improve protection of endangered residential areas and infrastructure. Therefore the purpose of this study was to summarize existing rockfall models and to propose modifications to make them suitable for predicting rockfall at a regional scale. First, the basic mechanics of rockfall are summarized, including knowledge of the main modes of motion: falling, bouncing and rolling. Secondly, existing models are divided in three groups: (1) empirical models, (2) process-based models and (3) Geophysical Information System (GIS)-based models. For each model type its basic principles and ability to predict rockfall runout zones are summarized. The final part is a discussion of how a model for predicting rockfall runout zones at a regional scale should be developed. A GIS-based distribution model is suggested that combines a detailed process-based model and a GIS. Potential rockfall source areas and falltracks are calculated by the GIS component of the model and the rockfall runout zones are calculated by the process-based component. In addition to this model, methods for the estimation of model parameters values at a regional scale have to be developed.

Key words: distributed model, GIS, modelling, natural hazard, rockfall.

I Introduction

In mountainous areas rockfall is a daily occurrence. The unpredictability of the frequency and magnitude of rockfall potentially endangers human lives and infrastructure. There are numerous examples of infrastructure destroyed or people killed by rockfall (e.g., Porter and Orombelli, 1980; Bunce *et al*., 1991; Badger and Lowell, 1992). To protect endangered residential areas and infrastructure, it is necessary to assess the risk posed by rockfall.

Rockfall is a relatively small landslide confined to the removal of individual and superficial rocks from a cliff face (Selby, 1982). Rockfall can generate large-scale mass

Tel., +31-20-5257420; fax, +31-20-5257431; e-mail, l.dorren@science.uva.nl

 10.1191/0309133303pp359ra

movements of rock material, but these processes are defined as rockslides or rock avalanches (see also Abele, 1994; Cruden and Varnes, 1996). Very occasionally, rockfall initiates catastrophic debris streams, which are even more dangerous (Hsü, 1975). Distinct evidences of rockfall are talus slope deposits at the foot of steep cliff faces, but rockfall also occurs on slopes covered with vegetation where evidence is less distinct.

Protective measures against rockfall can be taken by, for example, constructing catch or barrier fences and restraining nets (Hearn *et al.*, 1992; Spang and Sponser, 1995; Peila *et al.*, 1998), but these measures are expensive and they deteriorate with time. In some cases the maintenance of forest stands with an explicit protection function, or a protection forest, is cost-effective and more sustainable (Kienholz and Mani, 1994; Motta and Haudemand, 2000). However, in many mountainous regions it is not known whether active forest management ensures effective protection against rockfall.

One way to investigate the efficacy of a protection forest against rockfall is to carry out field experiments by throwing rocks through different types of forests and monitoring the number of rocks stopped by the forest. Unfortunately, this method is time- and labour-consuming, especially if it is required to assess the efficacy of all the protection forests throughout large mountainous areas. An alternative is to simulate falling rocks through forests using computer models. The large goal of using such modelling approaches is to predict rockfall activity and assess the function of forests for protecting human lives and infrastructure at a regional scale.

As a means of reaching this large goal the purpose of this literature study was to summarize the requirements for a model that predicts the risk posed by individual falling rocks at a regional scale. To reach this objective, three questions have to be answered. First, what are the main mechanics of rockfall? Secondly, which rockfall models have already been developed and tested? Thirdly, what are the components of existing models that predict rockfall runout zones at a regional scale? This review is structured on the basis of these three questions. Finally, the required components for a regional scale rockfall model will be discussed.

II Rockfall mechanics

1 Causes of rockfall

Rockfall starts with the detachment of rocks from bedrock slopes, which is mostly a cliff face in the case of a rockfall source area. All bedrock slopes are subject to various degrees of weathering, which may lead to fracturing, opening of joints and therefore to promotion of rockfall. The degree of rockfall promotion depends on the environmental factors causing physical and chemical weathering, and on the bedrock type (Schumm and Chorley, 1964; Day, 1997). Apart from the weathering rates, trigger mechanisms also determine whether rockfall occurs or not. In the literature, a wide range of rockfall trigger mechanics and conditions have been already described. These rockfall trigger mechanics can actually be divided into rockfall promoters and causes of the actual start of movement. However, in reality it is difficult to make a distinction between promoters and actual causes of rockfall, since often a certain process promotes weathering and causes rockfall, such as frost shattering. The slope morphology and the direct surrounding of the potential falling rock are the most important factors determining whether a rock could fall.

A well-known promoter and cause of rockfall is frost–thaw activity (Grove, 1972; Porter and Orombelli, 1980, 1981; Coutard and Francou, 1989; McCarrol *et al*., 1998; Matsuoka and Sakai, 1999). Gardner (1983) observed rockfall in the Canadian Rocky Mountains and concluded also that rockfall occurs especially on glacially oversteepened rock slopes that are exposed to alternating freezing and thawing. These rockfalls were low magnitude, high frequency events, which is typical for rockfall in alpine areas (Matsuoka and Sakai, 1999; Hungr *et al*., 1999; Jomelli and Francou, 2000). Douglas (1980) also studied low magnitude, high frequency rockfalls in Ireland and also found strong indications of frost-induced rockfall. However, Douglas (1980) stated that geotechnical properties of the bedrock material also played an important role. This is consistent with the results of Luckman (1976), who showed that rockfall is controlled by both the morphological and geological character of the cliff and rock surface temperature fluctuations.

Zellmer (1987), Bull *et al*. (1994) and Vidrih *et al*. (2001) described another cause of rockfall. They investigated the relationship between rockfall and seismic activity and concluded that rockfall was activated by seismic activity. Wieczorek *et al*. (1995, 2000) reported that rockfalls in the Yosemite valley were caused by different factors, such as earthquakes, rain storms, rapid snow melt, freeze–thaw cycles of water in joints, root penetration and wedging, or stress relief following deglaciation. They documented about 400 slope movements, among which rockfalls and rockslides have been more numerous than other types of slope movement. In about half the reports on slope movements, the trigger was either unreported or unrecognized. The reported events show that large winter rainstorms, rapid snowmelt and earthquakes triggered more movements than did freeze–thaw conditions or human activities (Wieczorek and Jäger, 1996).

Human activities leading to decreased stability of hill slopes in hard rock are still a minor factor compared with geological factors, but locally it can be of great importance, for example undercutting of slopes during quarrying or excavations for infrastructure (Selby, 1982). In addition, animals can cause rockfall, for example chamois climbing steep cliff faces.

This overview shows that various factors were reported as causes of rockfall but, in most cases, a combination of topographical, geological and climatological factors and time determine whether rockfall occurs.

2 Modes of motion of falling rocks

After the rock has been detached and starts to move, it descends the slope in different modes of motion. These modes of motion strongly depend on the mean slope gradient (Figure 1). The three most important modes of motion are freefall through the air, bouncing on the slope surface and rolling over the slope surface. In the following sections these modes of motion will be described in detail.

a Freefall of rocks: Freefall of rocks occurs on very steep slopes. According to Ritchie (1963) freefall occurs if the slope gradient below the potential falling rocks exceeds 76°,

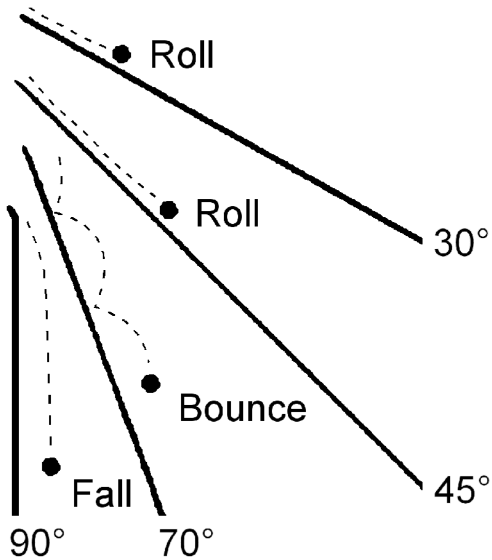

Figure 1 General modes of motion of rocks during their descent on slopes related to the mean slope gradients (modified from Ritchie, 1963 with permission of the Transport Research Board)

but in different field situations this value varies, therefore Figure 1 shows that around 70° the motion of the rock gradually transforms from bouncing to falling.

During freefall of rocks two different movements can occur. The first is translation of the centre of rock and the second is rotation of the block around its centre (Azzoni *et al.*, 1995). Translation and rotation are important, because falling rocks are hardly ever round. Following rotation in the air a rock can jump onto a different direction after impact compared with preceding directions.

Air friction influences the velocity of a freefalling rock, but according to Bozzolo and Pamini (1986) the air friction has no significant effect on the motion of the rock. Another influencing factor on freefalling rocks and their fall tracks is collision with other falling rocks, but these effects are hard to analyse during rockfall events or field investigations (Azzoni *et al.*, 1995).

b Movement at or near the slope surface: If the mean slope gradient decreases in the down-slope section, a rock collides on the slope surface after freefalling, which is defined as bouncing. During the first bounce rocks tend to break, especially incompetent rocks (Bozzolo and Pamini, 1986). Whether or not a rock breaks, 75–86% of the energy gained in the initial fall is lost in that first impact (Broilli, 1974; Evans and Hungr, 1993).

If the mean slope gradient is less than approximately 45°, a bouncing rock gradually transforms its motion to rolling because the rock gathers rotational momentum. A rolling rock is almost constantly in contact with the slope surface (Hungr and Evans, 1988). During the transition between bouncing and rolling, the rock rotates very fast and only the edges with the largest radius maintain contact with the slope. Thereby the centre of gravity moves along an almost straight path, which is an effective mode of motion with respect to energy loss. In fact, this combination of rolling and short bounces is one of the most economic displacement mechanisms (Erismann, 1986). Sliding is another mode of motion over the slope surface, but this generally only occurs in the initial and final stages of a rockfall. If the mean slope gradient increases, a sliding rock starts falling, bouncing or rolling. If the mean slope gradient does not change while sliding, the rock usually stops because of energy loss due to friction (Bozzolo and Pamini, 1986).

c Retardation of moving rocks: After different modes of motion a moving rock stops. The velocity and therefore stopping of a falling rock mainly depends on the mean slope gradient, since falling rocks generally accelerate on steeper slopes and decelerate on flatter slopes. But apart form the mean slope gradient the velocity also depends on the size of the rock and on the material covering the slope such as soil, scree and vegetation.

Small rocks retard more easily than bigger rocks; first, because during a rockfall the total kinetic energy of small rocks is lower than that of bigger rocks, secondly large obstacles such as trees can more easily stop small rocks, thirdly, small rocks retard more easily in depressions between larger rocks on talus slopes. These are the main causes of the sorting effect on talus slopes (Kirkby and Statham, 1975; Statham, 1976; Statham and Francis, 1986). Fine material is found near the base of the rock face and down slope the average rock size increases. The biggest rocks are mostly found near the base of the talus slope (Evans and Hungr, 1993). On alpine talus slopes this sorting effect is neither linear nor fully exponential. Generally, the sorting effect only accounts for the upper part of the talus slope, since avalanches deposit boulders with variable rock sizes mainly at the base of talus slopes (Jomelli and Francou, 2000).

Stopping of rocks is an abrupt rather than a gradual process. Stopping occurs because energy is lost through collisions and friction forces that act on the rock during transport over slope surfaces. The friction force of a moving rock is not only dependent on the rock shape, but also on the surface characteristics of the slope (Statham and Francis, 1986). Slope surface characteristics can vary a lot within short distances. Therefore the friction force between a rock and the slope surface can best be characterized by a dynamic angle of friction (Kirkby and Statham, 1975). The dynamic angle of friction is related to the surface roughness (Chang, 1998), which can be defined as the variation in height perpendicular to the slope within a certain slope distance (Pfeiffer and Bowen, 1989). Kirkby and Statham (1975) defined the dynamic angle of friction for a falling rock as,

$$\tan \phi_{\mu d} = \tan \phi_0 + k * d \ / \ (2 * R) \qquad (1)$$

where, $\phi_{\mu d}$ is dynamic angle of friction (°); ϕ_0 is angle of internal friction (°) (between 20.3° and 33.8°); k is a constant (between 0.17 and 0.26); d is mean diameter of scree on the slope surface (m); R is radius of the rock (m).

With respect to scree transport on slopes, much research has been done to investigate transport mechanisms and deposition rates (Kirkby and Statham, 1975; Statham, 1976; Carson, 1977; Statham and Francis, 1986; Blijenberg, 1995; Hétu and Gray, 2000; Jomelli and Francou, 2000). However, there is little quantitative information available on the effect of forest cover on the transport of scree or large rocks.

Jahn (1988) carried out one of the few quantitative studies on the effect of forest cover on rockfall and concluded that three to ten times as many falling rocks were stopped on forested slopes compared with similar slopes without a forest cover. Zinggeler *et al.* (1991) also investigated the importance of trees in stopping falling rocks and concluded that topography is just as important; falling rocks lose energy by colliding with tree stems, which eventually results in stopping on flatter areas in the terrain. Hétu and Gray (2000) observed the effect of forest on scree transport on slopes. They related an increased rock concentration along forest fringes on talus slopes to an increased forest density. According to them, there is a constantly ongoing battle between active talus slope development and forest colonization. The active front zone of the talus slope displaces downslope if a forest is disturbed by a large-scale mass movement or fire. This study indicated that forests cannot stop the devastating effect of large magnitude rockfall events, but for low magnitude–high frequency rockfall events forest provide effective protection. Still, much is unknown about the quantitative effect of forest cover on rockfall.

III Comparison of rockfall models

There are many different models for calculating runout zones of rockfall events. All existing rockfall models can be categorized in three main groups: (1) empirical models, (2) process-based models and (3) GIS-based models. The basic principles of each group of models and some examples will be described in this section.

1 Empirical models

Empirical rockfall models are generally based on relationships between topographical factors and the length of the runout zone of one or more rockfall events. Sometimes these models are referred to as statistical models (Keylock and Domaas, 1999). Tianchi (1983) established two relationships on the basis of recorded data from 76 major rockfalls. One relationship is an inverse logarithmic correlation between the volume of the rockfall and the ratio of the maximum vertical drop to the maximum horizontal distance travelled. The second relationship is a positive logarithmic correlation between the volume of the rockfall and the area covered by the fallen mass. On the basis of the two correlations Tianchi (1983) developed a model for a preliminary estimate of the extent of a threatening rockfall, if the volume can be estimated. Moriwaki (1987) did a comparable study and found a relationship between the angle of a line connecting the toe with the crown of the rupture and, first, the ratio of the maximum vertical drop to the maximum horizontal distance travelled and, secondly, the landslide volume.

Toppe (1987) and Evans and Hungr (1993) suggest the *Fahrböschung* principle (Heim, 1932) to predict run out zones of rockfall events. The *Fahrböschung* is the angle between a horizontal plane and a line from the top of a rockfall source scar to the stopping point for any given rockfall (Figure 2). It is important that the line follows the falltrack of the boulder. An alternative principle suggested by Evans and Hungr (1993) is the *minimum shadow angle*, following Lied (1977). This is the angle of a straight line between the highest point of the talus slope and the stopping point of the longest runout boulder for any given rockfall (Figure 2). Comparing the outcomes of several studies, the minimum

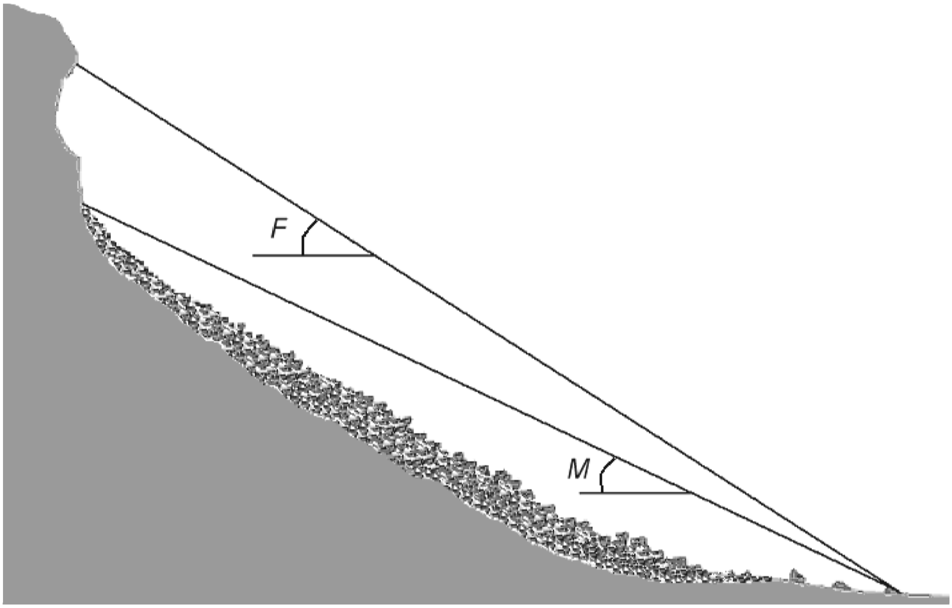

Figure 2 The *Fahrböschung* (*F*) and the *minimum shadow angle* (*M*) of a talus slope (modified from Meissl, 1998 with permission of the author)

shadow angle lies between 22° and 30° (Rapp, 1960; Govi, 1977; Lied, 1977; Hungr and Evans, 1988; Evans and Hungr, 1993). Evans and Hungr (1993) reported a *minimum shadow angle* of 27.5° after investigating 16 talus slopes in British Columbia. According to them, the *minimum shadow angle* is preferable to the *Fahrböschung*, but both should only be used for a first approximation of the length of a rockfall runout zone.

Keylock and Domaas (1999) tested three empirical models on their ability to predict the maximum length of rockfall runout zones using simple topographic parameters. The models were tested using rockfall data presented by Domaas (1994). Their first model was the *height function model*. This model assumes that the runout distance beyond the foot of the talus slope can be derived from the combined vertical height of the free rock face and the talus slope. Their second model was the *α-β model* following Heim (1932), Hsü (1975) and Körner (1976, 1980). The *α-β model* is based on the correlation between the average energy of an extreme rockfall event, where a boulder stops beyond the foot of the talus slope and the energy of an average event, where the boulder stops at the foot of the talus slope. Their third model was the *runout ratio* model, which is based on a model for estimating snow avalanche travel distance developed by McClung and Lied (1987). The *runout ratio model* describes the ratio between the horizontal length of the runout zone to the combined horizontal length of the talus slope and the free rock face. After statistical analysis of the model results and the field data on rockfall events presented by Domaas (1994), the most accurate model of the three tested by Keylock and Domaas (1999) appeared to be the *runout ratio model*.

2 Process-based models

Process-based models describe or simulate the modes of motion of falling rocks over slope surfaces. Kirkby and Statham (1975) and Statham (1976) developed a process-based rockfall model for transport of rocks over talus slopes, assuming that rocks only slide over a talus slope surface. The model results were compared with results of laboratory experiments. The model first calculated the velocity of the falling rock at the base of the cliff, following,

$$v = \sqrt{2 * g * h} \tag{2}$$

where, v is velocity (m s^{-1}); g is acceleration due to gravity (9.81) (m s^{-2}); and h is fall height (m).

On the basis of this velocity, the component of the fall velocity parallel or tangential to the slope surface was calculated, assuming that this component of the velocity is being conserved during the first impact of the rock on the slope surface. Finally the stopping position was calculated by the ratio of the fall velocity and a frictional force, which was determined by the dynamic angle of friction (see section II, 2, c).

Keylock and Domaas (1999) developed the *simple dynamics rockfall model*, which is a process-based model based on the model of Kirkby and Statham (1975). The *simple dynamics rockfall model* was tested using rockfall data presented by Domaas (1994). Their model calculated the travel distance over the slope surface on the basis of the friction force according to Kirkby and Statham (1975) and the acceleration due to gravity. On the basis of calculated exceedance probabilities of modelled rockfall travel distances, Keylock and Domaas (1999) concluded that the *simple dynamics rockfall model* did not appear to hold a significant advantage over the empirical models tested in their study.

In addition to the models of Kirkby and Statham (1975) and Keylock and Domaas (1999), there is a large group of process-based models that are rather similar (Wu, 1985; Bozzolo and Pamini, 1986; Hungr and Evans, 1988; Bozzolo *et al.*, 1988; Pfeiffer and Bowen, 1989; Kobayashi *et al.*, 1990; Evans and Hungr, 1993; Budetta and Santo, 1994; Chen *et al.*, 1994; Azzoni *et al.*, 1995, Chau *et al.*, 1998). Three factors correspond in all these models. First, these process-based models are two-dimensional slope-scale models that restricted falling boulders to move in a vertical plane. Consequently, lateral movements were not simulated. Secondly, the rockfall track was defined as a composite of connected straight lines with a slope angle equal to the measured mean slope gradient on the represented segment of the rockfall track as visualized in Figure 3.

Finally, motions were simulated as a succession of flying phases and contact phases. The flying phase was simulated with a parabola equation based on the initial velocity in x and y directions and the acceleration due to gravity. The collision point of the rock on the slope surface was calculated with the intersection of the parabolic flying function and the straight slope segments.

The first difference between these two-dimensional process-based models is that some of these models considered a falling rock with its mass concentrated in one point (Wu, 1985; Hungr and Evans, 1988; Pfeiffer and Bowen, 1989; Kobayashi *et al.*, 1990; Evans and Hungr, 1993), while other models considered the falling rock as an ellipsoidal body (Bozzolo and Pamini, 1986; Bozzolo *et al.*, 1988; Azzoni *et al.*, 1995).

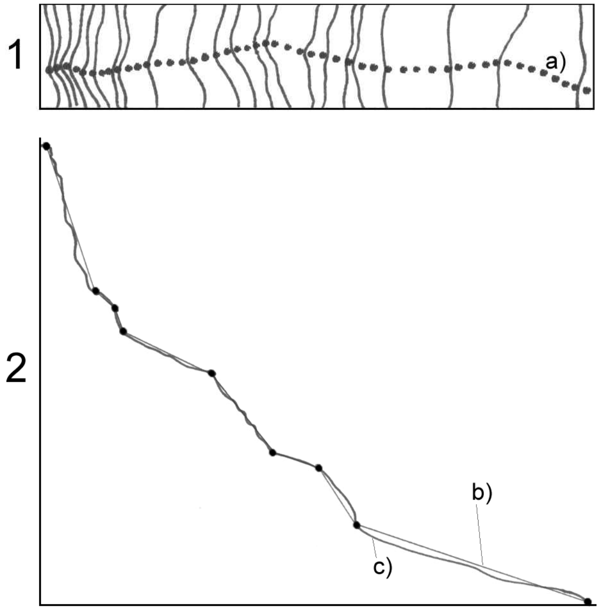

Figure 3 The upper figure (1) shows the actual rockfall path (a) projected on a contour line map. The lower figure (2) shows the slope segments (b) used in two-dimensional rockfall models representing the actual slope of the rockfall path (c)

Secondly, some models simulated the movement at or near the slope surface during a rockfall with detailed characterizations for bouncing, sliding and rolling (Bozzolo and Pamini, 1986; Kobayashi *et al.*, 1990; Evans and Hungr, 1993; Azzoni *et al.*, 1995), while other models considered bouncing, rolling and sliding as identical movements that can be described by a succession of impacts and bounces (Bozzolo *et al.*, 1988; Pfeiffer and Bowen, 1989). Models applying specific algorithms for calculating rolling and sliding velocities mainly used Coulomb's law of friction,

$$F_f = \mu_f * m * g * \cos\beta \tag{3}$$

where, F_f is friction force (tangential to the slope surface) (kg·m s^{-2}); μ_f is coefficient of friction; m is mass of the rock (kg); g is acceleration due to gravity (9.81) (m s^{-2}); ß is mean slope gradient (°).

The calculated friction force could then be used for calculating the sliding or rolling velocity of a rock after displacement over a given distance over the slope surface (Scheidegger, 1975; Bozzolo and Pamini, 1986; Hungr and Evans 1988; van Dijke and van Westen, 1990; Kobayahi *et al.*, 1990; Evans and Hungr, 1993; Azzoni *et al.*, 1995; Meissl, 1998). Here, the friction coefficient is the most determining factor for the velocity.

For calculating the velocity before and after a bounce, two principle approaches used in the two-dimensional process-based models referred to above can be identified. Both approaches calculated the velocity before and after a bounce on the basis of energy loss.

However, one approach defined energy loss by a coefficient for the efficiency of collision, which is the ratio of the total kinetic energy of the rock before and after the impact. The other approach calculated energy loss on the basis of a tangential coefficient of restitution that acts in a direction parallel to the slope surface and a normal coefficient of restitution that acts in a direction perpendicular to the slope surface.

Azzoni *et al*. (1995) developed a model based on the coefficient for the efficiency of collision. Their model was designed and calibrated with the experience and data gained from several field experiments in Italy. The model considered the falling rock as an ellipsoid (Figure 4) and simulated bouncing, sliding and rolling, based on the algorithms described by Bozzolo and Pamini (1986). Energy before and after the bounce was calculated on the basis of the angular velocity.

Azzoni *et al*. (1995) concluded that their model is generally able to make correct predictions of the fall velocities, bounce height and energy during the fall. They stated that their model results for predicting runout zones were acceptable, but unfortunately no accuracy values were given. Kobayashi *et al*. (1990) developed a model that simulated the contact phases with different characterizations for bouncing and rolling. Bouncing was also based on the coefficient for the efficiency of collision. Their model results were all within the 30% range of the measured rockfall runout zones and bounce marks. Errors were caused by collision with trees, loss of mass during falling and the smooth topography that was assumed in the model. Their main conclusion was that boulder shape is important in governing the modes of motion, but variations in topography control the mode of motion.

Pfeiffer and Bowen (1989) developed a model using both a tangential and normal coefficient for the efficiency of collision. Their model considered a falling rock with its

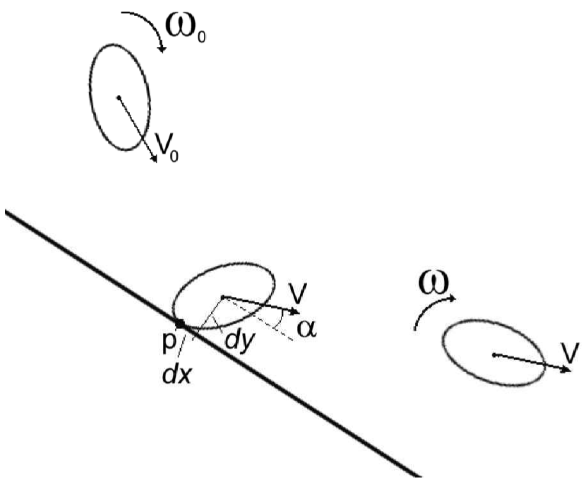

Figure 4 An ellipsoidal rock with initial angular velocity (ω_0) and initial velocity (v_0) continues its fall with angular velocity (ω) and velocity (v) after impact. The angle α is determined by the ratio of the tangential distance (dx) to the normal distance (dy) between the centre of the rock and impact point (p) (after Bozzolo and Pamini, 1986; Azzoni *et al*., 1995)

mass concentrated in one point. At each impact the incoming velocity of the rock was resolved into tangential (parallel to the slope) and normal (perpendicular to the slope) velocities. Both velocities changed because of energy loss defined by the tangential and the normal coefficient of restitution. The tangential coefficient of restitution was determined by the vegetation cover and the surface roughness. The normal coefficient of restitution was determined by elasticity of the surface material. The resultant of both outgoing velocity vectors is the velocity of the rock after bouncing on the slope surface. Rolling was simulated as a succession of impact and bouncing events.

Evans and Hungr (1993) described another example of a model that used the tangential and normal coefficient of restitution. They applied a lumped mass model to three test cases in British Columbia. In this model the rolling and the bouncing mode of motion was simulated separately. For every position on the slope the energy loss was calculated. If the ratio of the kinetic energy lost in an impact to the horizontal length of the corresponding bounce was larger than the rolling friction coefficient during three consecutive bounces, the model simulated a transition into the rolling mode, otherwise the rock continued with bouncing. The exact formula for the calculation of the rolling velocity was not given in their articles (Hungr and Evans, 1988; Evans and Hungr, 1993). Evans and Hungr (1993) concluded that their model requires much wider and thorough calibration, however, some encouraging results were already obtained.

Three-dimensional models for investigating rockfall at a slope scale were also developed (Descoudres and Zimmermann, 1987; Gascuel *et al.*, 1998). Descoudres and Zimmermann's (1987) model was developed and calibrated for analysing a rockfall in Wallis, Switzerland, where large blocks were involved (1–10 m^3). The model required a high resolution Digital Elevation Model (DEM), friction coefficients and coefficients for the plasticity and elasticity of the soil. A combined algorithm calculated both the falltrack and the velocity and produced satisfactory results for the test slope. Gascuel *et al.*'s (1998) model applied a bilinear interpolation to the input data to obtain continuous data coverage. On the basis of those interpolated data the model calculated detailed falltracks and velocities using friction coefficients and stress-deformation laws of rock and soil. Since model parameter values vary over the rockfall area and were therefore not perfectly known, the values for the parameters were stochastically changed during the simulation. Again this model produced satisfactory results for the test slope.

All the above-described process-based slope-scale models did not simulate multiple falling rocks and the complex interactions between them. Over the past decade progress has been made in the development of models that identify the coordinates, velocity and angular velocity for multiple particles in a three-dimensional space. These models simulate loss and gain of kinetic energy of particles as a result of inelastic and frictional collisions with each other and with the slope surface. These models were based on Discrete Element Methods (Donzé *et al.*, 1999; Okura *et al.*, 2000a,b) or on Discontinuous Deformation Analysis (Koo and Chern, 1998).

3 GIS-based models

GIS-based models are those either running within a GIS environment or they are raster-based models for which input data is provided by GIS analysis. GIS-based rockfall models consist of three procedures. The first procedure identifies the rockfall source areas in the region of interest, the second determines the falltrack and the third calculates the length of the runout zone (Hegg and Kienholz, 1995).

Meissl (1998) developed two GIS-based rockfall models using an empirical model for calculating the runout zone. The first model was *Schattenwinkel*. This model was based on the *minimum shadow angle* principle (Evans and Hungr, 1993), which is described in Section III, 1. The second model of Meissl (1998) was called *Geometrische Gefälle*. This model was based on the angle of the shortest line between the top of the rockfall source scar and the stopping point. Apart from these principles both models were identical, since both models used an identical module for calculating the falltrack and the source areas.

The falltrack module conducted a raster neighbourhood analysis using a 5×5 window. Therefore, this module was able to simulate 16 fall directions from a centre raster cell instead of eight directions (Figure 5), as in the commonly used D-8 method developed by O'Callaghan and Mark (1984). The falltrack module calculated the maximum height difference between the central raster cell and the 16 surrounding cells divided by the distance between the two cells. This analysis was referred to as the D-16 method (Meissl, 1998).

Both the *Schattenwinkel* and the *Geometrische Gefälle* model were tested on individual rockfall slopes. Only the *Schattenwinkel* model was tested for predicting rockfall runout zone at a regional scale. For this test, the rockfall source areas were derived from cliff faces on topographical maps or areas defined as endangering on geomorphological and geological maps. Unfortunately, the *Schattenwinkel* model could not handle the amount of required data (Meissl, 1998).

Other developed and tested models for rockfall hazard assessment at a regional scale were mainly GIS-based models using a process-based model for calculating the runout zone (see Van Dijke and van Westen, 1990; Meissl, 1998). These models can be defined as distributed models, since they are process-based and take into account the spatial

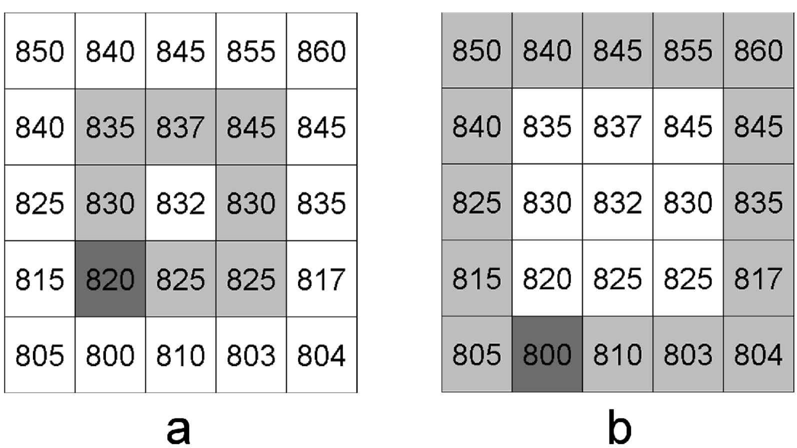

Figure 5 (a) D-8 method: fall direction from the central cell is towards the dark-grey cell if calculated with a 3×3 window. (b) Same example using a 5×5 window, which is used in the D-16 method of Meissl (1998)

variability within a certain region or catchment (Beven, 1985; Beven and Moore, 1993). In a GIS-based distributed rockfall model the terrain is represented by multiple rasters, which are derived from GIS data layers. Each raster represents a certain property of the terrain, for example, height above sea level, surface roughness, vegetation cover and geology.

Van Dijke and van Westen (1990) developed a distributed model that performs a neighbourhood analysis to a DEM derived from an isoline map with an equidistance of 20 m, representing an area of 80 km^2. A neighbourhood analysis calculated the fall direction for each raster cell. The direction was determined towards the neighbouring cell with the minimum height value. The velocity calculation of the model was based on an energy conservation principle as described by Scheidegger (1975). On the basis of this principle the velocity of the falling rock was calculated following,

$$v = \sqrt{v_0 + 2 * g * (h - \mu_f + X} \tag{4}$$

where, v is velocity of the falling rock (m s^{-1}); v_0 is initial velocity of the falling rock (m s^{-1}); g is acceleration due to gravity (9.81) (m s^{-2}); h is fall height (m); μ_f is coefficient of friction; X is distance travelled over the slope surface (m).

The velocity was calculated for each raster cell within the falltrack, starting at a potential rockfall source cell. Potential rockfall source cells were defined by the mean slope gradient (>60°). The value of the friction coefficient (μ_f) depended on the soil cover type, for example, bare rock, scree, residual soils, fluvial materials, dense forest and open forest. The model was tested for an area in the Austrian Alps by comparing the modelled results with detailed natural hazard maps of the area. The model results were compared with these maps. Van Dijke and van Westen (1990) concluded that their model was able to compute the general distributions of rockfall areas shown on their maps.

The GIS-based distributed model of Meissl (1998) was called *Sturzgeschwindigkeit*. This model simulated two different modes of motion: freefalling and sliding. The formula for the calculation of the velocity after freefalling is given in eq. (2). To account for energy loss during the first collision or bounce on the slope surface 75% of the velocity gained during the motion through the air was subtracted, following observations of Broilli (1974). In the following cells the model calculated a sliding velocity with the formula described in eq. (4).

Again, Meissl (1998) derived rockfall source areas from cliff faces on topographical maps or areas defined as endangering on geomorphological and geological maps. The falltrack was calculated with the D-16 method. *Sturzgeschwindigkeit* was tested for an alpine valley in Austria covering approximately 72 km^2. The terrain was represented using a DEM with a resolution of 50 m × 50 m. The outcomes of the model were compared with mapped rockfall patterns. From those comparisons, Meissl (1998) concluded that the simulated rockfall patterns on high altitudinal zones generally correspond with the mapped patterns, but unfortunately no model accuracies were given.

IV Synthesis: a GIS-based distributed rockfall model

As shown by many authors, models are widely used to predict the risk posed by rockfall, both at a slope scale and at a regional scale. In recent years rockfall models chiefly evolved towards three-dimensional and GIS-based models. A GIS-based model is favourable in case of predicting rockfall runout zones at a regional scale. GIS-based models require three procedures: one for identifying the rockfall source areas, the second for determining the falltrack and the third for calculating the runout zone.

A simple method for identifying rockfall source areas is defining thresholds for mean slope gradients (Toppe, 1987; van Dijke and van Westen, 1990). Another method is deriving rockfall source areas from cliff faces on topographical maps (Krummenacher, 1995; Meissl, 1998) or from areas defined as active rockfall slopes on geomorphological and geological maps (van Dijke and van Westen 1990). Another more realistic and automatic method is to identify rockfall source areas on the basis of a combined dataset in a GIS. This dataset could include: rock type, exposition, slope curvature, slope gradient and land cover.

The most common method used for determining a falltrack in GIS-based rockfall models is the D-8 method introduced by O'Callaghan and Mark (1984) or the D-16 method (Meissl, 1998). The advantage of the D-8 method is that the falltrack can be calculated cell by cell. Simultaneously the velocity of the falling block in every cell is calculated. In contrast, the D-16 method calculates the next position beyond the eighth neighbouring cells. Therefore, extra calculations have to be carried out to fill in the gaps in the raster (Meissl, 1998).

Another advantage of the D-8 method is its simplicity, which improves the speed of the computer simulation. A disadvantage of the D-8 method is the systematic error that occurs because of the restricted falltrack calculation (Figure 6), since rock movement is restricted to straight or diagonal directions. When applying the D-16 method the systematic error caused by this restriction decreases (Meissl, 1998). A point of concern for both methods is the fact that for each source cell only one direction is calculated, i.e., a rock in a given raster cell leaves by a single exit. Therefore a computer program using the D-8 or the D-16 method for determining the falltrack can never simulate the development of talus cones. The latter can be achieved by simulating lateral spreading of rocks from a single cell, using a multiple flow direction algorithm (Quinn *et al.*, 1991), or variations to this algorithm as summarized by Tarboton (1997).

For calculating rockfall runout zones, empirical or process-based models can be used. An empirical model results in a first approximation of rockfall runout zones. Process-based models seem to result in more accurate predictions of runout zones. Furthermore, an advantage of process-based models is that the interaction of falling rocks with tree stems or other barriers can be simulated. The main problem of rockfall modelling is calculating the bouncing and rolling velocity. Depending on the level of detail of the input data, more or less complex algorithms can be used. One possibility is to use a single coefficient for the efficiency of collision; another is to use both a normal and a tangential coefficient of restitution. In addition, an option is to use a separate algorithm for calculating the rolling velocity or to simulate rolling by a succession of impacts and bounces.

The tangential coefficient of restitution is determined by obstacles on the slope surface and the normal coefficient of restitution is determined by the elasticity of the

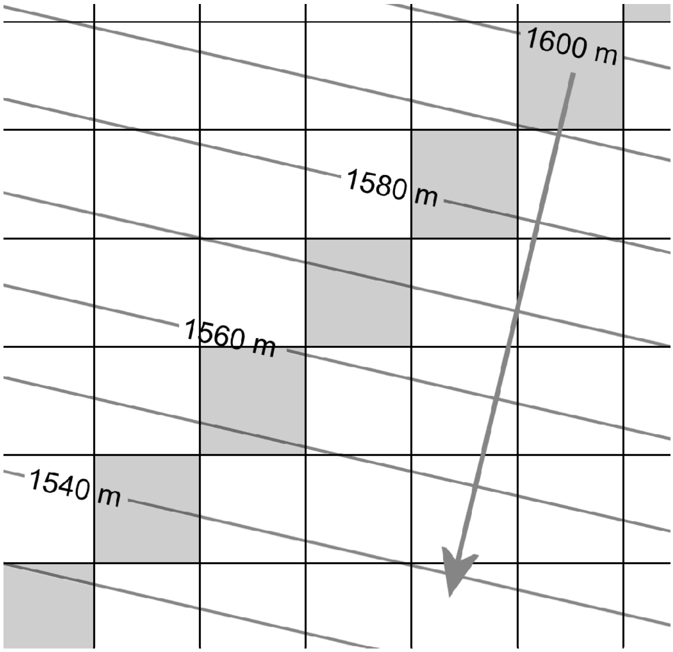

Figure 6 The arrow presents the actual falltrack on the slope depicted by the isolines. The direction deviates from the raster-based falltrack determined with the D-8 method, illustrated by the grey cells (after Meissl, 1998)

surface material. Therefore, the tangential and the normal coefficient of restitution are easier to estimate than a single coefficient for the efficiency of collision for certain slope parts. As a result the use of the tangential and the normal coefficient of restitution is preferred. Since the use of a separate algorithm for calculating the rolling velocity introduces another parameter that has to be estimated in the field (μ_f or the coefficient of friction), it is also preferred to simulate rolling by a succession of impacts and bounces. An alternative to the modelling approaches described above is to use models that are based on Discrete Element Methods (Donzé *et al.*, 1999; Okura *et al.*, 2000a,b) or on Discontinuous Deformation Analysis (Koo and Chern, 1998). However, these models require a larger amount of detailed data and are therefore not feasible for GIS-based models predicting rockfall runout zones at a regional scale.

An important condition for the calculation of rockfall runout zones using a GIS-based model is a DEM of the whole region of interest. To account for fine-scale topographic variability in the slope profiles, the preferred resolution of such a DEM is between 5 m × 5 m or 10 m × 10 m. However, a DEM for larger regions (e.g., >500 km^2) generally has a resolution of 25 m × 25 m or larger. The question is whether it is feasible to simulate freefalling, bouncing and rolling on the basis of input data with a resolution of 25 m × 25 m. With such a resolution realistic landscape details are lost, which could imply that the process is simulated accurately but the resulting pattern is not. The study by Meissl (1998) gave a preliminary answer to this question, since the GIS-based distributed model tested produced promising results. In contrast, the empirical GIS-based model was not suitable for a regional assessment of rockfall hazard at all. Nevertheless, if input data with a resolution of 25 m × 25 m is used, the input values should be varied stochastically to account for terrain variability.

Errors observed in the outcomes of the process-based and GIS-based distributed rockfall models were mainly caused by the variability in topography and by the variability in surface characteristics (Kobayashi *et al*., 1990; Meissl, 1998). In addition, inadequate characterization of the vegetation cover explained some errors (Kobayashi *et al*., 1990). These observations indicate that more research effort is required for assessing input data parallel to the development of a GIS-based distributed model for predicting rockfall runout zones at a regional scale. Combining geomorphological and geological maps, forest inventories and remotely sensed data within a GIS could provide the required data for the terrain characterization at a regional scale.

V Conclusions

Currently, a large variety of empirical and process-based rockfall models exist. Empirical models provide a quick and simple approximation of rockfall runout zones. Process-based models produce more accurate predictions of runout zones. In addition, process-based models seem to be most suitable for application in areas other than the areas the models were developed and calibrated for. Until now many process-based models were developed for specific slopes where rockfall causes problems, but only few models were applied for predicting rockfall runout zones at a regional scale. For predicting rockfall runout zones at a regional scale, the integration of process-based models and a GIS is promising. Three procedures are crucial for this approach: first, the identification of source areas, secondly, the determination of falltracks and thirdly, the calculation of the rockfall velocity that determines the length of the runout zones. Apart from developing and testing these three procedures, research should focus on the development of methods for an accurate characterization of the terrain at a regional scale. This is required for the estimation of model parameter values and for incorporating the effect of forests on rockfall runout zones. The latter is still underdeveloped in rockfall modelling.

Acknowledgements

I wish to thank A.C. Seijmonsbergen, J. de Vente and J.H.N. Versfelt for helpful comments on the submitted manuscript.

References

Abele, G. 1994: Large rockslides: their causes and movement on internal sliding planes. *Mountain Research and Development* 14(4), 315–20.

Azzoni, A., Barbera, G.L. and **Zaninetti, A.** 1995: Analysis and prediction of rockfalls using a mathematical model. *International Journal of Rock Mechanics and Mining Science* 32, 709–24.

Badger, T.C. and **Lowell, S.M.** 1992: Rockfall control in Washington State, rockfall prediction and control and landslide case histories. *Transportation Research Record* 1343, 14–19.

Beven, K. 1985: Distributed models. In Anderson, M.G. and Burt, T.P., editors, *Hydrological Forecasting*. Chichester: John Wiley & Sons

Ltd, 405–35.

Beven, K.J. and **Moore, I.D.** 1993: *Terrain analysis and distributed modelling in hydrology*. Advances in hydrological processes. Chichester: Wiley.

Blijenberg, H.M. 1995: In-situ strength tests of coarse, cohesionless debris on scree slopes. *Engineering Geology* 39(3), 137–46.

Bozzolo, D. and **Pamini, R.** 1986: Simulation of rock falls down a valley side. *Acta Mechanica* 63, 113–30.

Bozzolo, D., Pamini, R. and **Hutter, K.** 1988: Rockfall analysis – a mathematical model and its test with field data. *Proceedings of the 5th International Symposium on Landslides in Lausanne*, Rotterdam: Balkema, 555–60.

Broilli, L. 1974: Ein Felssturz in Großversuch. *Rock Mechanics* Suppl. 3, 69–78.

Budetta, P. and **Santo, A.** 1994: Morphostructural evolution and related kinematics of rockfalls in Campania (southern Italy): a case study. *Engineering Geology* 36, 197–210.

Bull, W.B., King, J., Kong, F.C., Moutoux, T. and **Phillips, W.M.** 1994: Lichen dating of coseismic landslide hazards in alpine mountains. *Geomorphology* 10(1), 253–64.

Bunce, C.M., Cruden, D.M. and **Morgenstern, N.R.** 1991: Assessment of the hazard from rock fall on a highway. *Canadian Geotechnical Journal* 34, 344–56.

Carson, M.A. 1977: Angles of repose, angles of shearing resistance and angles of talus slopes. *Earth Surface Processes* 2, 363–80.

Chang, W.R. 1998: The effect of surface roughness on dynamic friction between neolite and quarry tile. *Safety Science* 29(2), 89–108.

Chau, K.T., Wong, R.H.C. and **Lee, C.F.** 1998: Rockfall problems in Hong Kong and some new experimental results for coefficient of restitution. *International Journal of Rock Mechanics and Mining Science* 35(4), 662–63.

Chen, H., Chen, R. and **Huang, T.** 1994: An application of an analytical model to a slope subject to rockfall. *Bulletin of the Association of Engineering Geologists* 31(4), 447–58.

Coutard, J.P. and **Francou, B.** 1989: Rock temperature measurements in two alpine environments: implications for frost shattering. *Arctic and Alpine Research* 21, 399–416.

Cruden, M.D. and **Varnes, J.D.** 1996: Landslide types and processes. In Turner, A.K. and Schuster, R.L., editors, *Landslides: investigation and mitigation*. Washington DC: Transport Research Board, 36–75.

Day, R.W. 1997: Case studies of rockfall in soft versus hard rock. *Environmental and Engineering Geoscience* 3(1): 133–40.

Descoeudres, F. and **Zimmermann, T.** 1987: Three-dimensional dynamic calculation of rockfalls, In Herget, G. and Vongpaisal, S., editors, *Proceedings of the Sixth International Congress on Rock Mechanics*. Montreal. Rotterdam: Balkema, 337–42.

Domaas, U. 1994: Geometrical methods of calculating rockfall range. *NGI Report 585910-1*. Oslo: Norwegian Geotechnical Institute.

Donzé, F., Magnier, S.A., Montani, S. and **Descoeudres, F.** 1999: Numerical study of rock block impacts on soil-covered sheds by a discrete element method, *5ème Conférence Nationale en Génie Parasismique, AFPS'99*, Cachan.

Douglas, G.R. 1980: Magnitude frequency study of rockfall in Co. Antrim, North Ireland. *Earth Surface Processes and Landforms* 5, 123–29.

Erismann, T.H. 1986: Flowing, rolling, bouncing, sliding, synopsis of basic mechanisms. *Acta Mechanica* 64, 101–10.

Evans, S.G. and **Hungr, O.** 1993: The assessment of rockfall hazard at the base of talus slopes. *Canadian Geotechnical Journal* 30, 620–36.

Gardner, J.S. 1983: Rockfall frequency and distribution in the Highwood Pass area, Canadian Rocky Mountains. *Zeitschrift für Geomorphologie* 27(3), 311–24.

Gascuel, J.-D., Cani-Gascuel, M.-P., Desbrun, M., Leroi, E. and **Mirgon, C.** 1998: Simulating landslides for natural disaster prevention. In Arnaldi, B. and Hegron, G., editors, *Computer animation and simulation '98*. Proceedings of the Eurographics Workshop, Lisbon, 31 August–1 September 1998. Springer Verlag, 1–12.

Govi, M. 1977: Photo-interpretation and mapping of the landslides triggered by the Friuli Earthquake (1976). *Bulletin of the International Association of Engineering Geology* 15, 67–72.

Grove, J.M. 1972: The incidence of landslides, avalanches and floods in western Norway during the Little Ice Age. *Arctic and Alpine Research* 4, 131–38.

Hearn, G., Barret, R.K. and **McMullen, M.L.** 1992: CDOT Flexpost rockfall fence development, testing, and analysis. Rockfall Prediction and Control and Landslide Case Histories. *Transportation research record 1343*. Washington DC: National Academy of Sciences, 23–29.

Hegg, C. and **Kienholz, H.** 1995. Determining paths of gravity-driven slope processes – the 'Vector Tree Model'. In Carrara, A. and Guzetti, F., editors, *Geographic information systems in assessing natural hazards*. Dordrecht: Kluwer Academic Publishers, 79–92.

Heim, A. 1932: Bergsturz und Menschenleben. *Beiblatt zur Vierteljahrschrift der Naturforschenden Gesellschaft in Zürich* 77, 218 pp.

Hétu, B. and **Gray, J.T.** 2000: Effects of environmental change on scree slope development throughout the postglacial period in the Chic-Choc Mountains in the northern Gaspé Peninsula, Québec. *Geomorphology* 32(3), 335–55.

Hsü, K.J. 1975: Catastrophic debris streams (Sturzstroms) generated by rockfalls. *Geological Society of America Bulletin* 86, 129–40.

Hungr, O. and **Evans, S.G.** 1988. Engineering evaluation of fragmental rockfall hazards. *Proceedings of the 5th International Symposium on Landslides in Lausanne*. Rotterdam: Balkema, 685–90.

Hungr, O., Evans, S.G. and **Hazzard, J.** 1999: Magnitude and frequency of rock falls and rock slides along the main transportation corridors of southwestern British Columbia. *Canadian Geotechnical Journal* 36(2), 224–38.

Jahn, J. 1988: Entwaldung und Steinschlag. In *Proceedings of the International Congress Interpraevent 1988*. Bnd 1, Graz, 185–98.

Jomelli, V. and **Francou, B.** 2000: Comparing the characteristics of rockfall talus and snow avalanche landforms in an Alpine environment using a new methodological approach: Massif des Ecrins, French Alps. *Geomorphology* 35(3), 181–92.

Keylock, C. and **Domaas, U.** 1999: Evaluation of topographic models of rockfall travel distance for use in hazard applications. *Arctic, Antarctic, and Alpine Research* 31(3), 312–20.

Kienholz, H. and **Mani, P.** 1994: Assessment of geomorphic hazards and priorities for forest management on the Rigi north face, Switzerland. *Mountain Research and Development* 14(4), 321–28.

Kirkby, M.J. and **Statham, I.** 1975: Surface stone movement and scree formation. *Journal of Geology* 83, 349–62.

Kobayashi, Y., Harp, E.L. and **Kagawa, T.** 1990: Simulation of rockfalls triggered by earthquakes. *Rock Mechanics and Rock Engineering* 23, 1–20.

Koo, C.Y. and **Chern, J.C.** 1998: Modification of the DDA method for rigid block problems. *International Journal of Rock Mechanics and Mining Science* 35(6), 683–93.

Körner, H.J. 1976: Reichweite und Geschwindigkeit von Bergstürzen und Fliessschneelawinen. *Rock Mechanics* 8, 225–56.

—— 1980: The energy-line method in the mechanics of avalanches. *Journal of Glaciology* 26, 501–505.

Krummenacher, B. 1995: Modellierung der Wirkungsräume von Erd- und Felsbewegungen mit Hilfe Geographischer Informationssysteme (GIS). *Schweizerischen Zeitschrift für Forstwesen* 146, 741–61.

Lied, K. 1977: Rockfall problems in Norway. *ISMES Publication no. 90*, Bergamo, 51–53.

Luckman, B.H. 1976: Rockfalls and rockfall inventory data, some observations from Surprise valley, Jasper national park, Canada. *Earth Surface Processes* 1, 287–98.

Matsuoka, N. and **Sakai, H.** 1999: Rockfall activity from an alpine cliff during thawing periods. *Geomorphology* 28(3), 309–28.

McCarroll, D., Shakesby, R.A. and **Matthews, J.A.** 1998: Spatial and temporal patterns of late Holocene rockfall activity on a Norwegian talus slope: a lichenometric and simulation-modeling approach. *Arctic and Alpine Research* 30(1), 51–60.

McClung, D.M. and **Lied, K.** 1987: Statistical and geometrical definition of snow avalanche runout. *Cold Regions Science and Technology* 13, 107–19.

Meissl, G. 1998: Modellierung der Reichweite von Felsstürzen. Fallbeispeile zur GIS-gestützten Gefahrenbeurteilung aus dem Beierischen und Tiroler Alpenraum. Innsbrucker Geografischen Studien 28. Ph.D. Thesis, Universität Innsbruck, Innsbruck, 249 pp.

Moriwaki, H., 1987. Geomorphological prediction of the travel distance of a debris. *The China–Japan field workshop on landslide*. Xian-Lanzhou, China, 79–84.

Motta, R. and **Haudemand, J.-C.** 2000: Protective forests and silvicultural stability. An example of planning in the Aosta valley. *Mountain Research and Development* 20(2), 74–81.

O'Callaghan, J.F. and **Mark, D.M.** 1984: The extraction of drainage networks from digital elevation models. *Computer Vision, Graphics and Image Processing* 28, 323–44.

Okura, Y., Kitahara, H. and **Sammori, T.** 2000a: Fluidization in dry landslides. *Engineering Geology* 56(3), 347–60.

Okura, Y., Kitahara, H., Sammori, T. and **Kawanami, A.** 2000b: The effects of rockfall volume on runout distance. *Engineering Geology* 58(2), 109–124.

Peila, D., Pelizza, S. and **Sassudelli, F.** 1998: Evaluation of behaviour of rockfall restraining nets by full scale tests. *Rock Mechanics and Rock Engineering* 31(1), 1–24.

Pfeiffer, T.J. and **Bowen, T.D.** 1989: Computer simulation of rockfalls. *Bulletin of the Association of Engineering Geologists* XXVI(1), 135–46.

Porter, S.C. and **Orombelli, G.** 1980: Catastrophic rockfall of September 12, 1717 on the Italian flank of the Mont Blanc Massif. *Zeitschrift für Geomorphologie N.F.* 24, 200–18.

—— 1981: Alpine rockfall hazards. *American Scientist* 69(1), 67–75.

Quinn, P., Beven, K., Chevallier, P. and **Planchon, O.** 1991: The prediction of hillslope flow paths for distributed hydrological modelling using digital terrain models. *Hydrological Processes* 5(1), 59–79.

Rapp, A. 1960: Recent development of mountain slopes in Kårkevagge and surroundings, northern Scandinavia. *Geografiska Annaler* 42, 65–200.

Ritchie, A.M. 1963: Evaluation of rockfall and its control. *Highway Research Record* 17, 13–28. Washington, DC: Highway Research Board, National Research Council.

Scheidegger, A.E. 1975: *Physical aspects of natural catastrophes*. Amsterdam / New York: Elsevier.

Schumm, S.A. and **Chorley, R.J.** 1964: The fall of endangering rock. *American Journal of Science* 262, 1041–54.

Selby, M.J. 1982: *Hillslope materials and processes*. New York: Oxford University Press.

Spang, R.M. and **Sönser, T.** 1995: Optimized rockfall protection by 'ROCKFALL'. In Fuji, T., editor, *Proceedings of the 8th International Conference on Rock Mechanics*. 25–30 September 1995. Rotterdam: A.A. Balkema, Tokyo, 1233–42.

Statham, I. 1976: A scree slope rockfall model. *Earth Surface Processes* 1, 43–62.

Statham, I. and **Francis, S.C.** 1986: Influence of scree accumulation and weathering on the development of steep mountain slopes. In Abrahams, A.D., editor, *Hillslope processes*. Winchester: Allen and Unwin Inc., 245–67.

Tarboton, D.G. 1997: A new method for the determination of flow directions and upslope areas in grid digital elevation models. *Water Resources Research* 33(2), 309–19.

Tianchi, L. 1983: A mathematical model for predicting the extent of a major rockfall. *Zeitschrift für Geomorphologie* 27(4), 473–82.

Toppe, R., 1987. Terrain models – a tool for natural hazard mapping. In Salm, B. and Gubler, H., editors, *Avalanche formation, movement and effects*. IAHS Publication no. 162, 629–38.

van Dijke, J.J. and **van Westen, C.J.** 1990: Rockfall hazard, a geomorphological application of neighbourhood analysis with ILWIS. *ITC Journal* 1, 40–44.

Vidrih, R., Ribičič, M. and **Suhadolc, P.** 2001: Seismogeological effects on rocks during the 12 April 1998 upper Soča Territory earthquake (NW Slovenia). *Tectonophysics* 330(3), 153–75.

Wieczorek, G.F. and **Jäger, S.** 1996: Triggering mechanisms and depositional rates of postglacial slope-movement processes in the Yosemite Valley, California. *Geomorphology* 15, 17–31.

Wieczorek, G.F., Nishenkod, S.P. and **Varnes, D.J.** 1995: Analysis of rockfalls in the Yosemite Valley, California. In Daemen, J.J.K. and Schultz, R.A., editors, *Rock mechanics: proceedings of the 35th US symposium*. Rotterdam: Balkema, 85–89.

Wieczorek, G.F., Snyder, J.B., Waitt, R.B., Morrissey, M.M., Uhrhammer, R.A., Harp, E.L., Norris, R.D., Bursik, M.I. and **Finewood, L.G.** 2000: Unusual July 10, 1996, rock fall at Happy Isles, Yosemite National Park, California. *Geological Society of America Bulletin* 112(1), 75–85.

Wu, S.-S. 1985: Rockfall evaluation by computer simulation. *Transportation Research Record* 1031, 1–5.

Zellmer, J.T. 1987: The unexpected rockfall hazard. *Bulletin of the Association of Engineering Geologists* 24(2), 281–83.

Zinggeler, A., Krummenacher, B. and **Kienholz, H.** 1991: Steinschlagsimulation in Gebirgswäldern. *Berichte und Forschungen 3*. Geographisches Institut der Universität Freiburg, 61–70.